ARTICLE

www.the-innovation.org

A causal multiomics study discriminates the early immune features of Ad5-vectored Ebola vaccine recipients

Zhe Zhang,[1,4] Wenjing Yang,[2,4] Zhengshan Chen,[1,4] Haoang Chi,[3,2,4] Shipo Wu,[1] Wanru Zheng,[1] Ruochun Jin,[2] Busen Wang,[1] Yudong Wang,[1] Nan Huo,[1] Jinlong Zhang,[1] Xiaohong Song,[1] Liyang Xu,[2] Jun Zhang,[1] Lihua Hou,[1,*] and Wei Chen[1,*]

*Correspondence: houlihua@sina.com (L.H.); cw0226@foxmail.com (W.C.)

Received: July 7, 2023; Accepted: February 28, 2024; Published Online: March 2, 2024; https://doi.org/10.1016/j.xinn.2024.100603

GRAPHICAL ABSTRACT

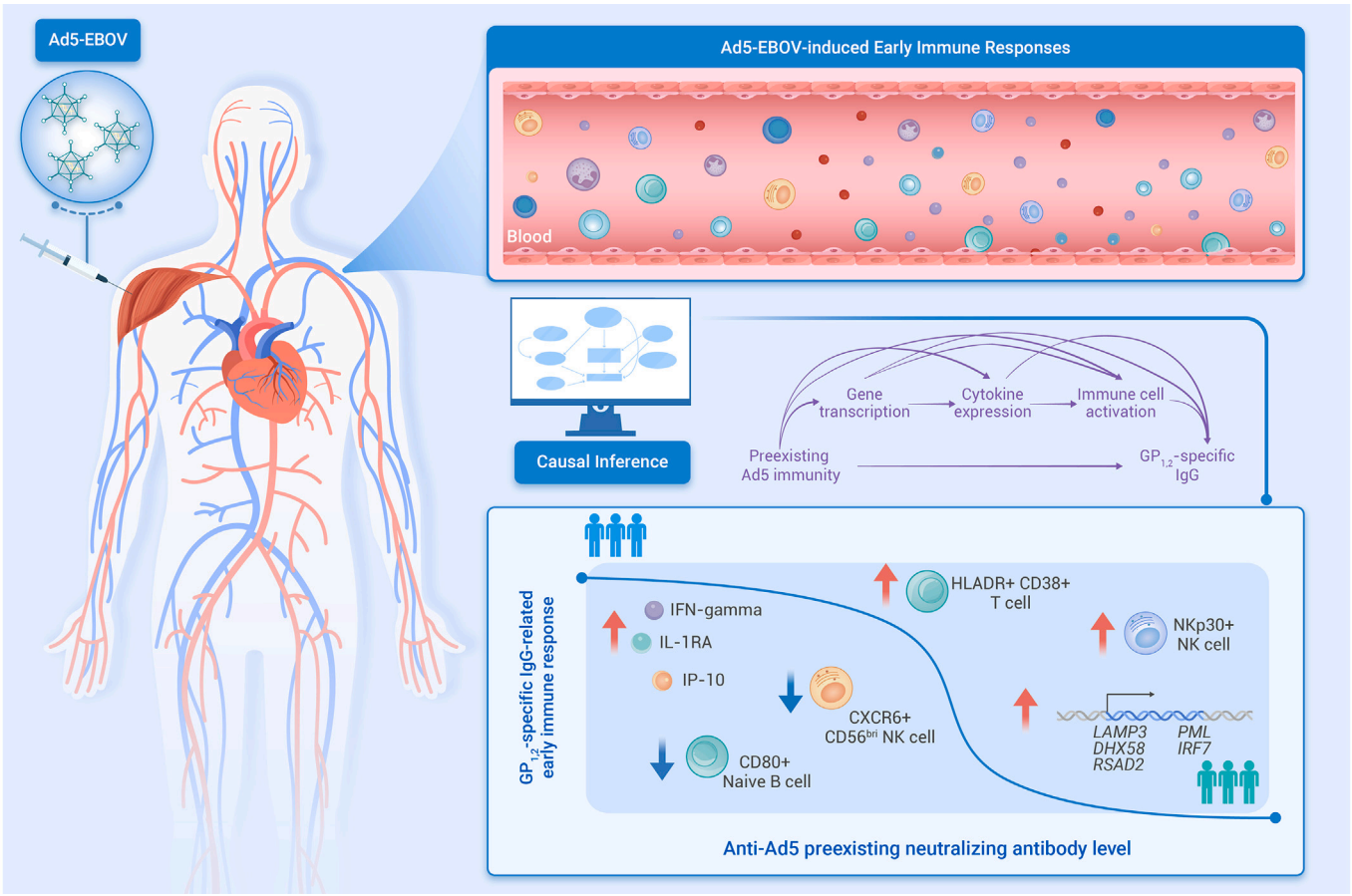

PUBLIC SUMMARY

- The increase in $GP_{1,2}$-specific IgG induced by Ad5-EBOV was strongly correlated with the development of early antiviral and inflammatory responses.
- Greater innate immune responses were elicited in Ad5-EBOV recipients with lower preexisting Ad5 immunity.
- A general causality-based tool was proposed to analyze multiomics vaccine immune responses.

ARTICLE

A causal multiomics study discriminates the early immune features of Ad5-vectored Ebola vaccine recipients

Zhe Zhang,[1,4] Wenjing Yang,[2,4] Zhengshan Chen,[1,4] Haoang Chi,[3,2,4] Shipo Wu,[1] Wanru Zheng,[1] Ruochun Jin,[2] Busen Wang,[1] Yudong Wang,[1] Nan Huo,[1] Jinlong Zhang,[1] Xiaohong Song,[1] Liyang Xu,[2] Jun Zhang,[1] Lihua Hou,[1,*] and Wei Chen[1,*]

[1]Institute of Biotechnology, Academy of Military Medical Sciences, Beijing 100071, China

[2]Department of Intelligent Data Science, College of Computer Science and Technology, National University of Defense Technology, Changsha 410073, China

[3]Intelligent Game and Decision Lab, Academy of Military Science, Beijing 100091, China

[4]These authors contributed equally

*Correspondence: houlihua@sina.com (L.H.); cw0226@foxmail.com (W.C.)

Received: July 7, 2023; Accepted: February 28, 2024; Published Online: March 2, 2024; https://doi.org/10.1016/j.xinn.2024.100603

Citation: Zhang Z., Yang W., Chen Z., et al., (2024). A causal multiomics study discriminates the early immune features of Ad5-vectored Ebola vaccine recipients. The Innovation **5(3)**, 100603.

The vaccine-induced innate immune response is essential for the generation of an antibody response. To date, how Ad5-vectored vaccines are influenced by preexisting anti-Ad5 antibodies during activation of the early immune response remains unclear. Here, we investigated the specific alterations in $GP_{1,2}$-specific IgG-related elements of the early immune response at the genetic, molecular, and cellular levels on days 0, 1, 3, and 7 after Ad5-EBOV vaccination. In a causal multiomics analysis, distinct early immune responses associated with $GP_{1,2}$-specific IgG were observed in Ad5-EBOV recipients with a low level of preexisting anti-Ad5 antibodies. This study revealed the correlates of the Ad5-EBOV-induced IgG response and provided mechanistic evidence for overcoming preexisting Ad5 immunity during the administration of Ad5-vectored vaccines.

INTRODUCTION

Adenovirus type 5 (Ad5) has been a common adenoviral vector for many vaccine development efforts due to its ability to elicit strong humoral and cellular immune responses.[1–3] In the past few decades, this vaccine platform has been widely used in preclinical and clinical trials for vaccines against several viruses causing infectious diseases, including Ebola virus,[4,5] Zika virus,[6] HIV,[7] and SARS-CoV-2.[8] Previous clinical studies have shown that participants vaccinated with a single dose of an Ad5-vectored vaccine usually generate adaptive immunity rapidly (within ~2 weeks), including antigen-specific antibodies and T cell responses.[9,10] To date, vaccines based on Ad5, Ad26, and the chimpanzee vector ChAd3, which express the Ebola glycoprotein ($GP_{1,2}$), have been approved for the prevention of Ebola virus disease due to their safety and potential to elicit robust immune responses in humans.[11] However, the immune response can be dampened in subjects with preexisting Ad5 immunity due to complex immune components, including Ad5 neutralizing antibodies (NAbs), Ad5-specific T cells, and type I interferon (IFN)-activated natural killer (NK) cells.[12] Several strategies have been developed to address this problem, such as modifying the viral vector,[13,14] altering the vaccine delivery approach,[15] and using adenovirus vectors of rare serotypes.[16] However, how the vaccine-induced systemic immune response is influenced by preexisting anti-Ad5 antibodies still needs to be better defined.

Successful activation of the innate immune system is essential for initiating vaccine-induced adaptive immune responses.[17] Within a few hours of entering the host, adenovirus vector vaccines can stimulate a cascade of innate immune signals through pathogen-associated molecular patterns and pattern recognition receptors on cells.[18] Innate immune cells are programmed to elicit rapid and robust antiviral transcriptional responses, accompanied by the expression of multiple cytokines and chemokines.[19] These diverse biological elements form immune features that assist in predicting vaccine-induced immune responses or immunotherapeutic effects.[20–22] Previous studies have shown that mucosal-associated invariant T cell activation is positively correlated with T cell responses induced by AZD1222, an adenovirus-vectored vaccine against SARS-CoV-2. NK cell-derived IFN-γ and the expression of CD86 on $CD14^+$ monocytes are associated with vaccine-induced antibody responses. Given that early immune responses are complex and involve genes, cytokines, and cell subsets, system integration analysis using causal inference may facilitate an in-depth exploration of the immune response to vaccines.[23,24]

Here, we described the specific alterations in elements of the early immune response that were correlated with the Ad5-EBOV-induced immunoglobulin G (IgG) response at the genetic, molecular and cellular levels. Causal multiomics analysis allowed us to distinguish immune features between Ad5-Ebola vaccine (EBOV) recipients with different levels of preexisting anti-Ad5 antibodies. This study characterized the correlates of the Ad5-EBOV-induced IgG response and provided mechanistic evidence for overcoming preexisting Ad5 immunity during the administration of Ad5-vectored vaccines.

RESULTS

Preexisting Ad5 NAbs dampened the $GP_{1,2}$-specific IgG response induced by Ad5-EBOV

Thirty-six volunteers who had never been infected with the Ebola virus were included and received one intramuscular dose of Ad5-EBOV (8×10^{10} vp). Blood samples were collected on the indicated days before and after vaccination for various immunological analyses (Figure 1A). Volunteers were assigned to the HAC or LAC according to their preexisting Ad5 NAb titers. No significant difference was observed, although the Ad5 NAb titer slightly increased with age (Figure 1B). Adults aged 18–20, 21–30, 31–40, and older than 40 years had Ad5 neutralizing titers of 69, 444, 475, and 372, respectively. Similar results were found for the proportion of Ad5-seropositive rate (Figure 1C). All of the volunteers were positive for a $GP_{1,2}$-specific IgG response on day 28 after vaccination. We found that the $GP_{1,2}$-specific IgG response was marginally influenced by age and preexisting anti-Ad5 antibodies but not sex (Figures 1D–1F). The recipients older than 40 years had a relatively weak IgG response, with a GMT of 1,995 (95% confidence interval [CI] 1,099–3,621), whereas those aged 18–20 years had an IgG response, with a GMT of 2,863 (95% CI 2,006–4,084). The GMTs of $GP_{1,2}$-specific IgG in HAC and LAC were 2,166 (95% CI 1,537–3,054) and 2,952 (95% CI 2,261–3,855), respectively. In addition, a weak negative correlation without significant differences ($r = -0.1609$, $p = 0.3485$) between the titers of $GP_{1,2}$-specific IgG and Ad5 NAbs was found in the Ad5-EBOV recipients (Figure 1G). Together with our previous findings,[9] the preexisting Ad5 NAb response demonstrated an impact on the $GP_{1,2}$-specific IgG response induced by Ad5-EBOV.

The plasma cytokine profile activated temporarily by Ad5-EBOV is associated with the generation of an antibody response

Plasma was collected from recipients on days 0, 1, 3, and 7 after vaccination and subjected to analysis of multiple cytokines using the Luminex (xMAP) platform, which analyzed 38 analytes. Of these analytes, 10 showed significant changes, 14 showed no or marginal changes, and 14 were below the detection threshold. The cytokine profile in the plasma showed a rapid response to Ad5-EBOV (Figures 2A, 2B, and S1A). After vaccination, highly significant but transient increases in IFN-γ ($p = 0.0051$), IL-1RA ($p = 0.0042$), TNF-α ($p = 0.0185$), and other cytokines were observed on day 1 (Figure 2B). Notably, IP-10 levels were substantially increased on days 1 ($p < 0.0001$) and 3 ($p < 0.0001$) as compared to the background levels of IP-10. The cytokine responses returned to near-baseline levels 3–7 days after vaccination.

We further analyzed the differentially expressed cytokines in volunteers with different levels of Ad5 NAbs. Vaccination with Ad5-EBOV triggered a more obvious activated cytokine profile in LAC than in HAC on day 1 (Figure 2C). Specifically, significant increases in the levels of IFN-γ(3.5-fold, $p = 0.0091$), IP-10 (3.3-fold, $p < 0.0001$), and IL-1RA (2.3-fold, $p = 0.0070$) were detected in LAC (Figure 2D). In HAC, the levels of IP-10 and IL-1RA on day 1 were 2.2-fold ($p = 0.0005$) and 1.3-fold ($p = 0.0402$) greater than the levels observed at baseline, respectively. The levels of other cytokines, such as IL-10, MIP-1β, and TNF-α, were

slightly increased or barely altered in the volunteers regardless of the Ad5 NAb levels (Figure S1B). The cytokine response patterns of the two groups partially overlapped, with LAC exhibiting a clear separation from PC1 (Figure S1C).

Since Ad5-EBOV induced a cytokine signature featuring IFN-γ, IP-10, IL-10, and IL1-RA, the relationships between the alterations in these cytokines and the levels of $GP_{1,2}$-specific IgG were examined. We observed significant correlations, with multiple cytokines belonging to coexpression clusters on day 1 but not on days 3 or 7, indicating that a coordinated cytokine response during the early innate immunity stage was induced by Ad5-EBOV (Figure 2E). Compared to that in HAC, the cytokine response in LAC had a stronger correlation with the $GP_{1,2}$-specific IgG titer. In LAC, the concentrations of IFN-γ and IL-10 on day 1 were positively correlated with the $GP_{1,2}$-specific IgG titer on day 28 (IFN-γ and $GP_{1,2}$-specific IgG: r = 0.69, p = 0.0043; IL-10 and $GP_{1,2}$-specific IgG: r = 0.65, p = 0.0094) (Figure 2F). Similar correlations with antibody titers were found for IP-10 and IL-1RA in terms of fold changes (IP-10 and $GP_{1,2}$-specific IgG: r = 0.52, p = 0.0475; IL-1RA and $GP_{1,2}$-specific IgG: r = 0.49, p = 0.0657). In contrast, there was no obvious correlation between cytokine levels and the IgG response in HAC vaccinees. All of the selected cytokine markers were negatively correlated with the preexisting anti-Ad5 antibody titer (Figure S1D). These results suggest that a distinct cytokine response is elicited by Ad5-EBOV and plays an important role in supporting the $GP_{1,2}$-specific IgG response.

Ad5-EBOV induced varying degrees of lymphopenia and immune cell activation, which correlated with preexisting anti-Ad5 antibody levels

To characterize early Ad5-EBOV-induced innate immune responses, changes in the frequency and activation status of different immune cell populations, including myeloid dendritic cells (mDCs) and plasmacytoid dendritic cells (pDCs), monocytes, NK cells, B cells, and T cells, were explored before and after vaccination (Figure S2). The innate immune response was strongly activated on day 1 and gradually declined to baseline 3–7 days after vaccination (Figure 3A). At early time points, the subjects exhibited reduced NK cell and T cell responses and increased DC and monocyte responses. More robust changes were observed in LAC, in which the relative frequencies of monocytes and DCs increased from 10.4% to 27.0% and 3.5%–5.1%, whereas the frequencies of T cells and NK cells decreased from 69.5% to 56.1% and 15.3% and 10.1%, respectively. A stronger response was found in LAC than in HAC, regardless of the time point (Figure S3A). On day 1, 58 of 109 immune cell subsets showed significant responses. Noticeable increases in the frequency of multiple immune cell types with distinct surface markers, such as $CCR7^+$ mDCs and monocytes, $HLA\text{-}DR^+CD38^+$ CD4 T cells, and $CD69^+$ NK cells, were observed compared to baseline (Figure 3B). In contrast, the frequencies of nonclassical monocytes, $CCR7^+$ pDCs, and $CD86^+$ pDCs decreased after vaccination. These data suggested that Ad5-EBOV rapidly triggered a polarized early immune response to the vaccine in the peripheral blood.

To determine the critical roles of these innate immune cells in the induction of the $GP_{1,2}$-specific IgG response, correlations were calculated between the $GP_{1,2}$-specific titer and the immune cell response. The cell markers included both absolute (day 1) and relative (day 1/day 0) values for the immune cell frequency and the median fluorescence intensity (MFI) of surface markers. The levels of 23 cell markers were strongly related to the $GP_{1,2}$-IgG titer (Figure 3C). Most monocytes and T cell subsets, such as $CCR7^+$ classical monocytes and $CD4^+$ T cells, were positively related to the $GP_{1,2}$-specific IgG response, whereas $CD80^+$ naive B cells and $CXCR6^+$ NK cells exhibited an inverse correlation. PCA revealed substantial differences between LAC and HAC on day 1 (p = 0.005) compared with those on days 3 and 7, indicating that preexisting anti-Ad5 antibodies influenced the immune cell profiles (Figure 3D). These results showed that the presence of preexisting anti-Ad5 antibodies in subjects altered the early immune response induced by Ad5-EBOV.

Next, we identified the cell markers strongly linked to the $GP_{1,2}$-specific IgG-related cytokine profile. IP-10 correlated well with most cell markers, followed by IL-1RA and IL-10 (Figure 3E). Regarding the fold change in the concentration of IP-10 before and after vaccination, multiple activated T cell subsets had a positive correlation, but $CD80^+$ naive B cells had an inverse correlation. The percentage of KIR^+ NK cells show a distinct relationship with the concentration of IL-10 on day 1. The MFI of CXCR6 on CD56bri NK cells was associated with both IP-10 and IL-1RA levels, which were confirmed to correlate with the EBOV-induced $GP_{1,2}$-specific IgG response. Compared with HAC, Ad5-EBOV markedly regulated the expression of these cell markers in LAC (Figures 3F and S3B). These observations indicated that alterations in immune cell subsets in Ad5-EBOV recipients were accompanied by the changes in cytokine levels and prompted us to further examine transcriptome changes.

The innate antiviral transcriptional response peaks on day 1 and correlates with the Ad5-EBOV-elicited immune profile

Bulk mRNA sequencing was conducted on PBMCs sampled on days 0, 1, 3, and 7 after vaccination. The strongest transcriptional response induced by Ad5-EBOV was observed on day 1. The number of differentially expressed genes (DEGs) on day 1 was 12.67-fold and 5.14-fold greater than that on days 3 and 7, respectively, with more upregulation than downregulation (Figures 4A and S4A). The most unique DEGs were identified in LAC on day 1, and the most overlapping DEGs were found between LAC and HAC on day 1 (Figure S4B). The immune response modules were shown to be activated following GSEA, which was highly consistent with the observed changes in cytokines and innate immune cells (Figure 4B). Within 3 days postvaccination, genes enriched in the monocyte, DC, innate immune and antiviral response modules were activated. In contrast, the downregulated genes were strongly enriched in NK cell and T cell activation genes. On day 7, the activation of plasma and T cell-related genes was observed, representing the initiation of adaptive immunity.

Because the $GP_{1,2}$-specific IgG response is closely correlated with EBOV-mediated protection, we examined whether there were antibody-associated differences in the response to Ad5-EBOV vaccination. GSEA conducted after the DEGs on day 1 were ranked according to their correlations with the $GP_{1,2}$-specific IgG titers. The top three enriched modules were M75, M165, and M11.0, indicating the critical role of antiviral and innate responses in antibody generation (Figure 4C). The correlation between the enriched modules and the $GP_{1,2}$-specific IgG response suggested different patterns in LAC and HAC (Figures 4D and S4C). Compared to those in HAC, volunteers in LAC had a more robust overall correlation, with more genes associated with the IgG response. In these modules, the relative expression of genes on day 1 compared to baseline generally showed a positive correlation with IP-10 and IL-1RA levels and a negative correlation with the MFI of CXCR6 on $CXCR6^+CD56bri$ NK cells and $CD80^+$ naive B cells (Figure 4E). In addition, we found that genes strongly linked to antibody-related cytokines and cell subsets, especially genes in the M75 and M165 modules, had different expression levels in LAC and HAC (Figures 4F and 4G). Collectively, these data demonstrated that Ad5-EBOV activated innate immune and antiviral transcripts to shape the early immune response, which correlated with the humoral response.

Multiomics analysis via causal inference revealed the relationship between the early immune response and the $GP_{1,2}$-specific IgG response

To further explore causality, we used CMA to select the $GP_{1,2}$-specific IgG-related immune features in the gene, cytokine, and immune subset profiles and discover their activation mechanisms (causal dependencies) (Figure 5A). CMA was used to select the genes with obvious causal mediation effects from among all of the DEGs. According to previous statistical correlation-based methods, 5 of the 21 genes obtained were enriched in the top 2 modules. DExH-box helicase 58 (DHX58), IFN regulatory factor 7 (IRF7), PML, and radical *S*-adenosyl methionine domain containing 2 (RSAD2) belong to ANTIVIRAL IFN SIGNATURE (M75), and lysosomal associated membrane protein 3 (LAMP3) belongs to ENRICHED IN ACTIVATED DENDRITIC CELLS (II) (M165). We also identified BST2 and USP18, which belong to the VIRAL SENSING & IMMUNITY; IRF2 TARGETS NETWORK (I) (M111.0) (Figure 5B).

After identifying the genes that play important roles in the immune response, we further used CMA to discover which cytokines these genes affect to promote the $GP_{1,2}$-specific IgG response. We found that IFN-γ, IL-1RA, and IP-10 are critical for this process. These markers overlapped with the previously selected cytokine markers (IFN-γ D1, IL-10 D1, IP-10 D1/D0, and IL-1RA D1/D0). Therefore, our CMA helped us discover the mechanisms of action of genes and cytokines, supporting our previous results from another perspective. Furthermore, we used CMA to determine which immune cells affected these cytokines to directly promote the IgG response. We selected eight critical immune subsets as mediators of the correlation between the selected cytokines and the $GP_{1,2}$-specific IgG response. Compared to statistical correlation-based results, such as LAMP3 → IFN-gamma → $CD80^+$ naive B, DHX58 → IFN-γ → $CD80^+$ naive B, and RSAD2 → IFN-γ → $CD80^+$ naive B, we obtained similar correlation results and revealed the

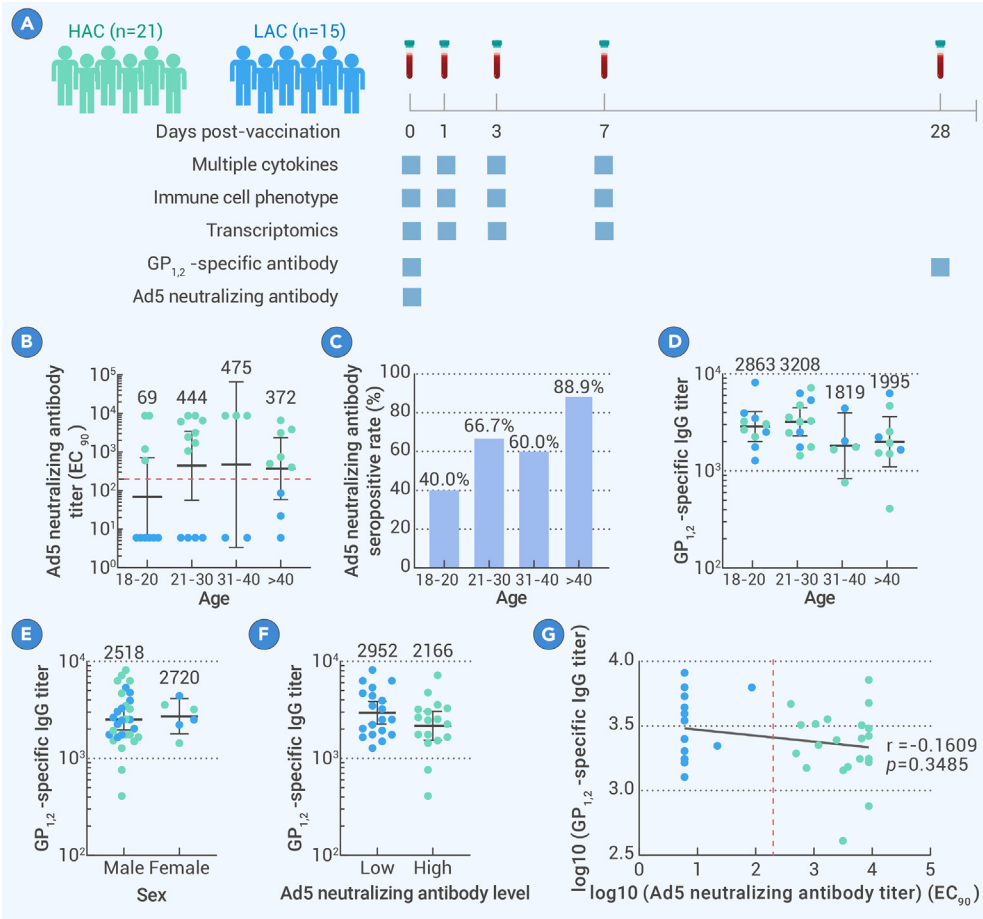

Figure 1. Antibody response in Ad5-EBOV recipients
(A) Schematic representation of the study design. (B and C) The titer (B) and seropositive rate (C) of Ad5-specific NAbs before vaccination in volunteers of different ages. (D–F) The titer of $GP_{1,2}$-specific IgG on day 28 after vaccination in volunteers of different ages (D), sexes (E), or preexisting Ad5 NAb levels (F). (G) Correlation between the $GP_{1,2}$-specific IgG titer on day 28 and the Ad5 NAb titer on day 0 after vaccination. The data in (B) and (D)–(F) are represented as the individual Ad5 or $GP_{1,2}$-specific antibody titer, with the error bars denoting 95% CIs and the connecting lines reflecting geometric means. The dashed lines in (A) and (G) indicate an Ad5 NAb titer of 200. Subjects were stratified by preexisting Ad5 NAb titers (green indicates subjects with a titer of >1:200, and blue indicates subjects with a titer ≤1:200).

specific underlying causal relationships. Thus, we investigated the causal relationships of antibody-related signatures via three omics approaches (Table S1).

DISCUSSION

Preexisting antibody immunity in the host usually negatively affects vaccine-induced immune effects. Relatively little is known about the features of the early immune response elicited by Ad5-vectored vaccines, with or without the influence of anti-Ad5 NAbs. The systematic investigation of early immune responses in vaccinees is beneficial for understanding vaccine activation mechanisms and predicting vaccine effectiveness. In this study, we conducted a causal inference-based multiomics analysis to integrate the dynamic responses of gene transcripts, plasma analytes, and cell subtypes in subjects at an early time point after Ad5-EBOV vaccination. We found that the vaccinees rapidly generated robust inflammatory and innate immune responses within 24 h after one intramuscular dose of Ad5-EBOV. Similar early responses were observed in participants injected with other virus-vectored vaccines, such as AdVac Malaria Vaccines and rVSV-EBOV.[25,26] In contrast, subjects vaccinated with mRNA vaccines often reached their peak innate response at an early time point after the second dose rather than after the initial dose.[27] The self-adjuvant properties of vector viruses can partially explain this difference. Viruses such as adenovirus can stimulate a cascade of innate immune signals through pathogen-associated molecular patterns and pattern-recognition receptors on host cells, thus activating antiviral and antigen presentation pathways, which are essential drivers of inflammation and innate immunity.[28,29] However, the early immune responses in subjects with a high level of preexisting anti-Ad5 antibody were substantially impaired, manifesting as a global attenuation of cytokine expression, cell activation, and gene transcription. This result is compatible with research data on an Ad5-based vaccine against HIV, which suggested that preexisting anti-Ad5 antibodies interact with Fc receptors on antigen-presenting cells and hinder the presentation of vaccine-encoded antigens.[30]

In recent years, increasing attention has been given to blood analytes due to their value in distinguishing disease and immune response signatures.[31] We dynamically monitored the responses of 38 plasma analytes and identified 10 cytokines/chemokines that exhibited significant changes in concentration. Most of these factors, including IL-15, IFN-γ, and IP-10, have been reported to be correlated with the adaptive immune response.[32,33] In addition, MCP-1, IL-10, IL-1RA, MIP-1β, and TNF-α were reported to be correlated with adverse events in Ebola and SARS-CoV-2 vaccine recipients.[34,35] We observed a tight network among these 8 cytokines/chemokines on day 1 after vaccination. Among these factors, IFN-γ, IP-10, IL-1RA, and IL-10 were confirmed to have a close connection with $GP_{1,2}$-specific IgG titers in LAC but not HAC. These cytokines are often released in the context of inflammation or immunomodulation. Thus, the preexisting anti-Ad5 NAb in the host impeded activation of the innate immune response, leading to reduced $GP_{1,2}$-specific IgG generation.

Similar to other vaccines and pathogens, Ad5-EBOV can trigger lymphopenia and the activation of innate immune cells in the peripheral blood. The responses of various $GP_{1,2}$-specific IgG-related immune subsets differed between LAC and HAC vaccinees. The frequency of $CCR7^+$ classical monocytes and the MFI of CXCR6 on $CXCR6^+$ CD56bri NK cells were noticeably altered on day 1 after vaccination in LAC. Reportedly, IFN-γ-experienced monocytes and $CXCR6^+$ NK cells are involved in vaccine-elicited early immune responses, which suggests that these cell types contribute to shaping the $GP_{1,2}$-specific IgG response.[27,36] Further phenotyping of lymphocytes revealed a response of $CD80^+$ naive B cells and $HLA\text{-}DR^+CD38^+CD4^+$ T cells that correlated with the expression of IP-10 in the plasma. The responses of these subsets showed a pattern that was opposite to those of their parent immune cells ($CD19^+$ B cells or $CD3^+$ T cells) and were influenced by preexisting anti-Ad5 antibodies. To date, the dynamics of these populations in humans have not been described in any previous study. Future research should investigate whether these subsets play a functional role in Ad5-EBOV-induced generation of an IgG response.

In this study, early gene transcription activity was highly consistent with the cytokine and immune cell profiles of Ad5-EBOV recipients. When we used the correlation with the IgG titer instead of the gene expression level, three modules related to antiviral and innate immune responses were selected for GSEA; these modules were similar to those induced by other vaccines.[37,38] Some of the enriched genes were strongly correlated with Ad5-EBOV-induced cytokine and immune subset profiles, and they were also reported to be among the transcripts that responded to Ebola virus infection. Furthermore, causal inference analysis confirmed that LAMP3, DHX58, RSAD2, PML, and IRF7 are involved in this process. Although none of them have been investigated as regulators of Ad5-vectored vaccines, the pattern recognition receptor DHX58 and the immune function-related factor LAMP3 are important for regulating the vaccine-induced adaptive immune response,[39,40] and RSAD2, PML, and IRF7 were found to have antiviral effects against various pathogens.[41–43] Further investigations into the functions of these proteins in the context of Ad5-vectored vaccines are needed.

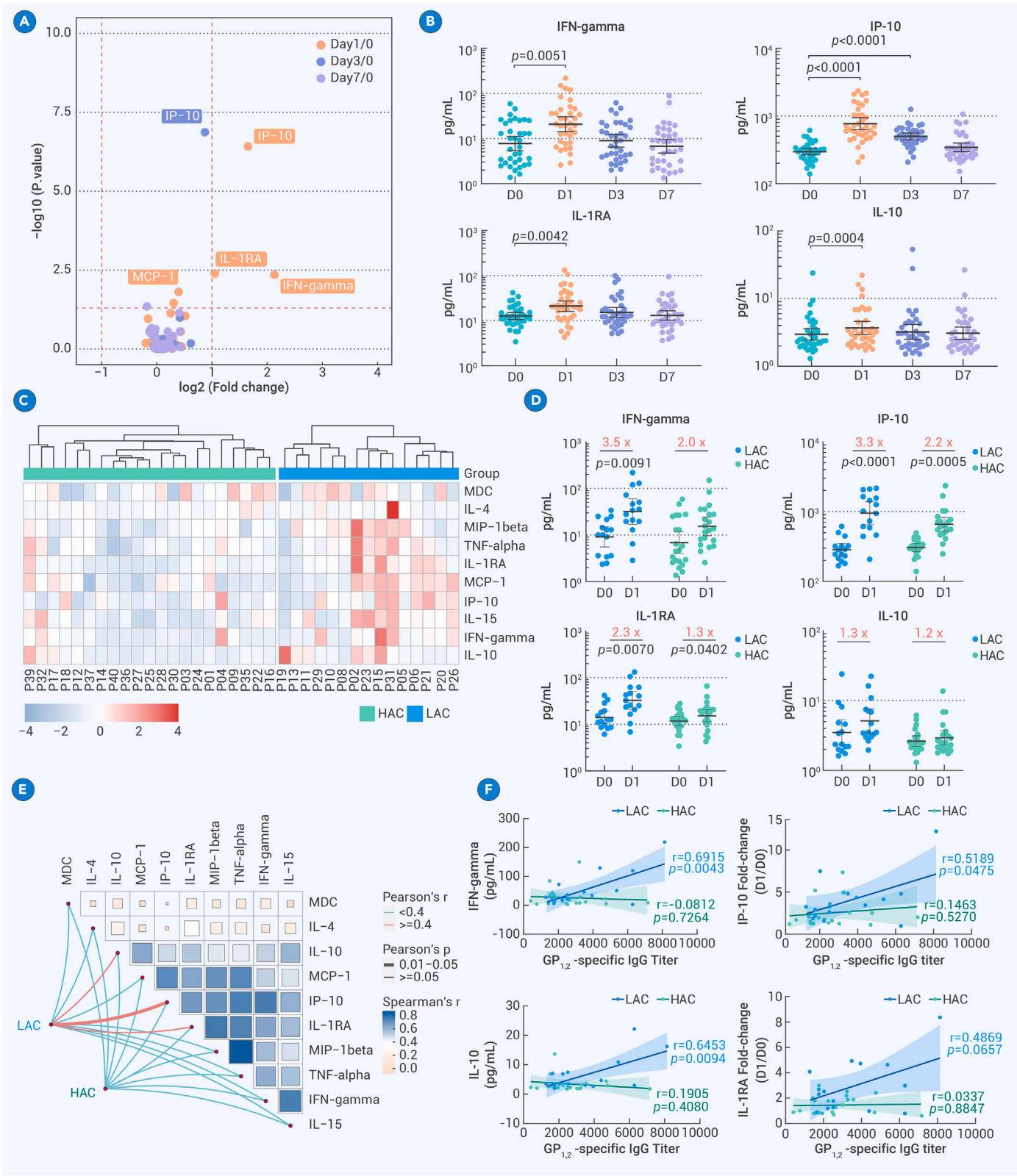

Figure 2. Cytokine profile induced by Ad5-EBOV The levels of multiple cytokines and chemokines were measured using the Luminex assay. (A) Volcano plots showing differentially expressed analytes on days 1, 3, and 7 in comparison to day 0 after vaccination. (B) The levels of IFN-γ, IP-10, IL-1RA, and IL-10 in the serum were plotted over time and showed changes after vaccination. (C) Heatmaps depicting the $\log_2$-fold changes of 10 differentially expressed analytes in LAC and HAC on day 1 after vaccination. (D) Comparison of changes in the serum concentrations of IFN-γ and IP-10 between LAC and HAC. The red numbers on the top are the fold changes in cytokine concentrations from days 0 to 1. (E) Pairwise comparisons of cytokine expression are shown, with a color gradient and filled areas denoting Spearman's correlation coefficients. Pearson's correlation coefficient between the $GP_{1,2}$-specific IgG titer on day 28 and relative cytokine expression on day 1 versus day 0 in LAC and HAC was calculated separately. The edge color corresponds to Pearson's r statistic, and the edge width denotes the statistical significance. (F) Pearson's correlations between the $GP_{1,2}$-specific IgG titer and the indicated cytokine markers, including the concentrations of IFN-γ and IL-10 on day 1, the fold changes in the IP-10 concentration, and the geometric concentration of IL-1RA from days 0 to 1. The data in (B) and (D) are represented as individual cytokine concentration values, with the error bars denoting 95% CIs and the connecting lines reflecting geometric means. Statistical significance was assessed using the Wilcoxon matched-paired signed rank test in (A) and (B) and using the Mann-Whitney test in (D).

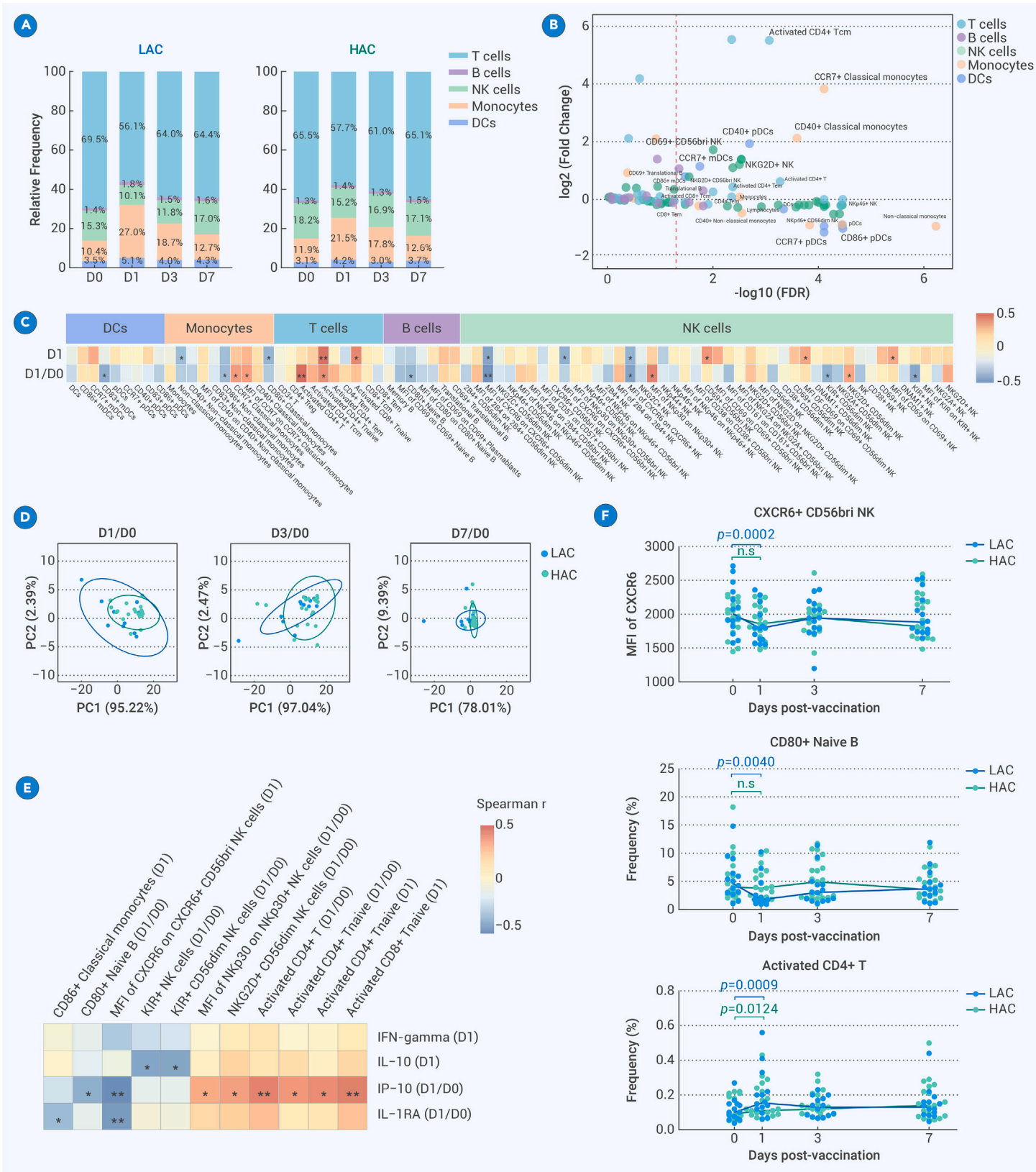

Figure 3. Flow cytometry analysis of multiple immune cell populations in the peripheral blood in response to Ad5-EBOV (A) The relative proportions of major immune cell populations on days 0, 1, 3, and 7 after vaccination in LAC and HAC. (B) Volcano plot showing changes in multiple immune cell populations in Ad5-EBOV recipients on day 1 relative to day 0. (C) Heatmap of the Spearman correlations between the responses of significantly activated immune cell populations on day 1 and $GP_{1,2}$-specific IgG titers on day 28 after vaccination. (D) PCA of the immune cell population response on days 1, 3, and 7 relative to day 0. Each dot represents a PBMC sample, color-coded according to the preexisting anti-Ad5 antibody level (see key). (E) Heatmap representations of the Spearman correlation matrix between selected immune cell markers and cytokine markers. (F) MFI of CXCR6 on $CXCR6^+$ NK cells, frequency of $CD80^+$ naive B cells, and frequency of activated $CD4^+$ T cells on days 0, 1, 3, and 7 after vaccination in LAC and HAC. The data in (F) are represented as individual immune cell response values, with the connecting lines representing the median frequency or fluorescence intensity at each indicated time. Statistical significance was assessed using the Wilcoxon matched-paired signed rank test in (F). *p < 0.05; ***p < 0.001; ns, not significant.

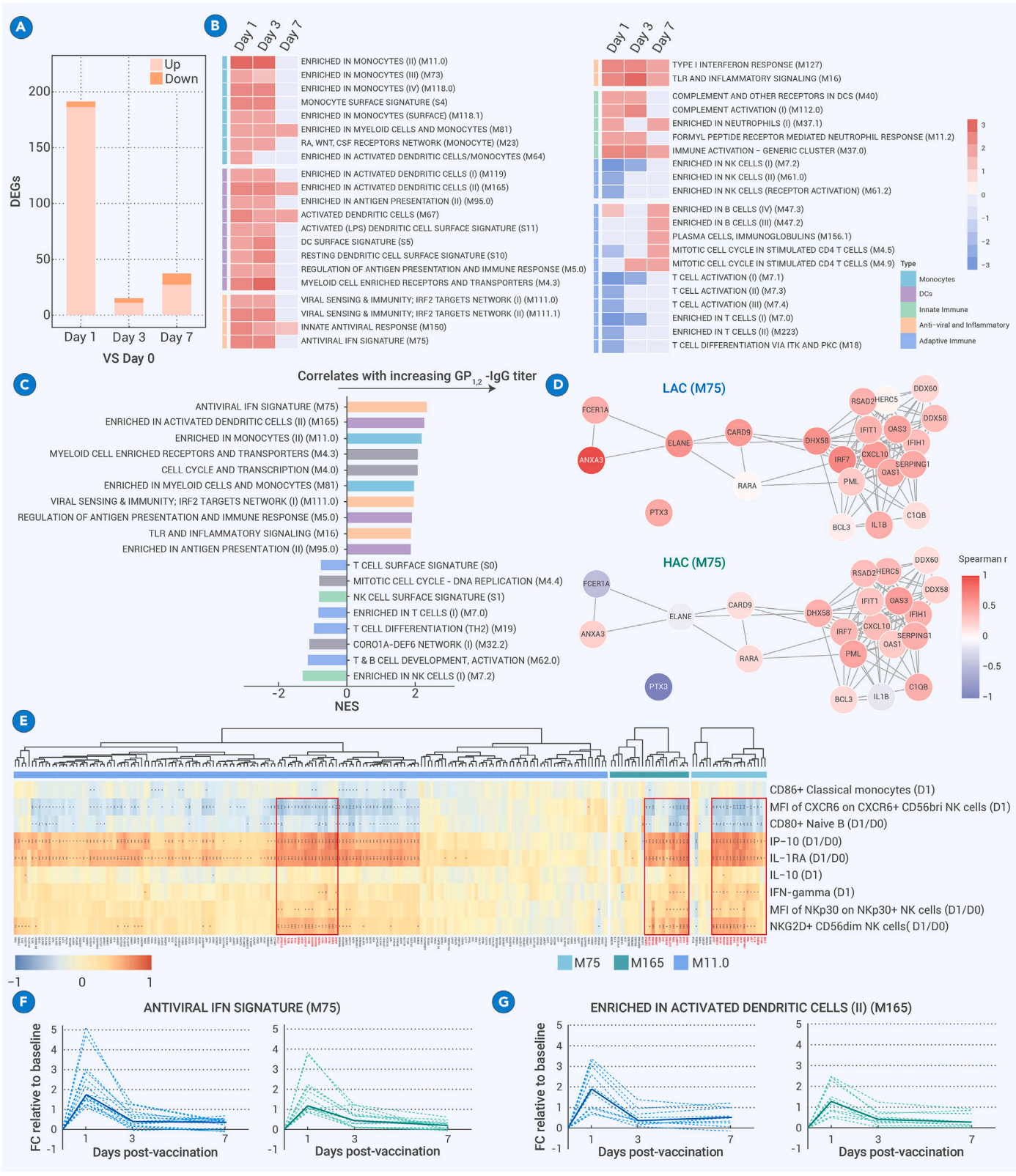

Figure 4. Transcriptional signatures after Ad5-EBOV vaccination (A) Number of DEGs (absolute log_2 fold change > 1 and FDR adjusted $p < 0.05$) at each time point after vaccination. (B) BTMs significantly enriched in the gene set from day 1 versus day 0, day 3 versus day 0, and day 7 versus day 0. (C) BTMs on day 1 that were significantly associated with $GP_{1,2}$-specific antibody titers. The gene list was ranked according to the correlation coefficients of day 28 $GP_{1,2}$-specific antibody titers and day 1/day 0-fold changes in genes. GSEA was used to evaluate the enrichment of BTMs within the gene list. (D) Correlations of genes (day 1 versus day 0, fold change) in M75, an antiviral BTM, with the $GP_{1,2}$-specific IgG titer on day 28. The color represents the Spearman correlation coefficient. Each edge (gray line) represents a co-reactive relationship (Spearman r > 0.5 and FDR adjusted $p < 0.05$) between genes (day 1 versus day 0, fold change). The LAC (top) and HAC (bottom) are shown separately. (E) Heatmap showing the Spearman correlations of cytokines/immune cell types and genes within modules M75, M165, and M11.0. (F and G) Temporal expression patterns of each gene within modules M75 (F) and M165 (G); bold lines represent the median fold change of all of the genes. The LAC (blue) and HAC (green) are shown separately.

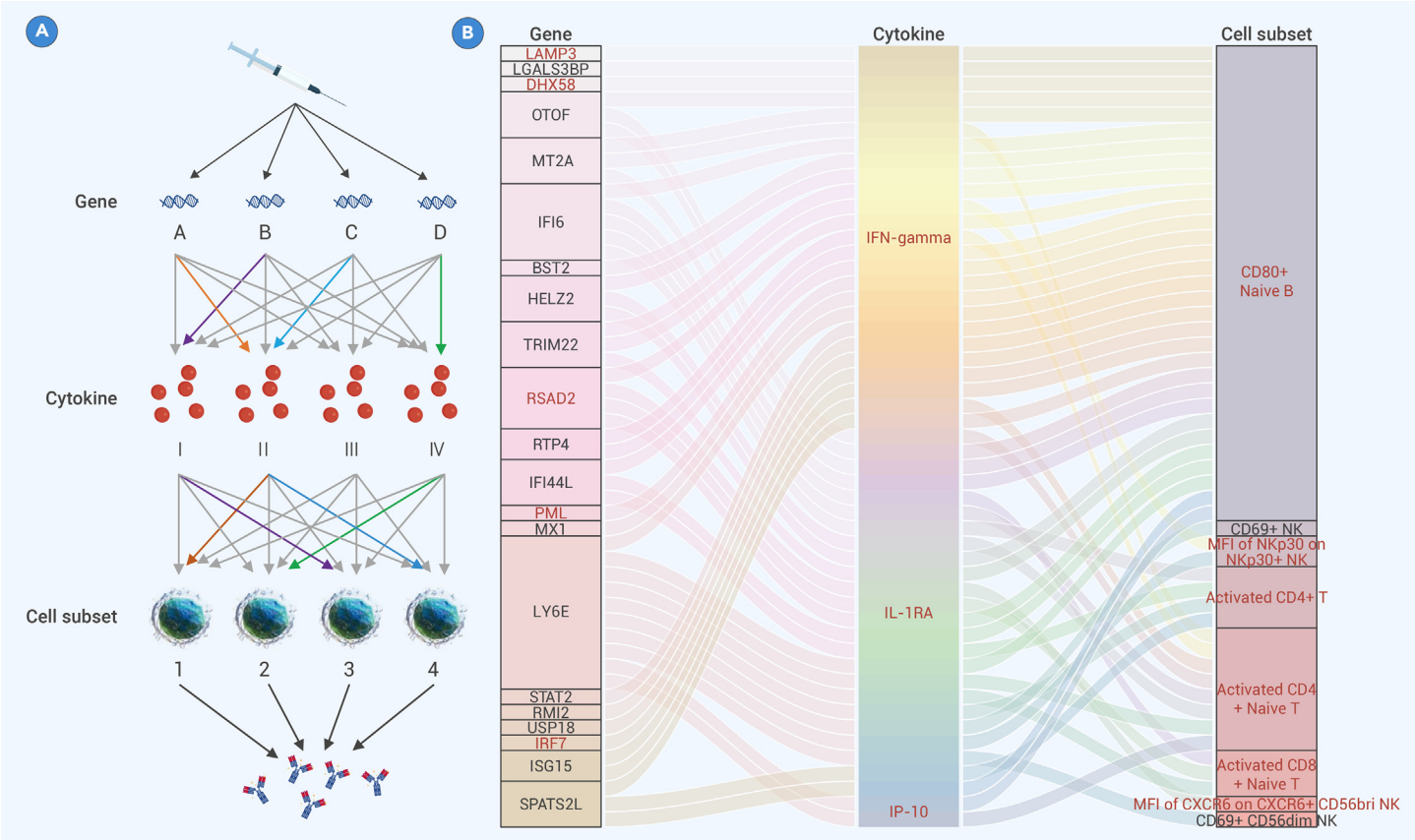

Figure 5. Multiomics study via causal inference analysis (A) A diagram of the immunologic mechanism (causal dependency) that we aimed to discover with 3 omics datasets. (B) Visualization of CMA of multiomics data for the early immune response. The left column shows the genes that clearly affect the $GP_{1,2}$-specific IgG response. The center column shows the cytokines induced by the genes on the left that have clear effects on the $GP_{1,2}$-specific IgG response. The right column shows the immune subsets induced by cytokines in the center column that have clear effects on the $GP_{1,2}$-specific IgG response. The connecting lines among these 3 omics datasets show the mechanism of action (i.e., causal dependency). The order from top to bottom for each column indicates the proportion of the mediation effect. The objects in red overlap with those in the previous correlation-based analysis.

Due to the complexity of the human immune system,[44] many unexpected confounding factors may negatively affect the results obtained with correlation-based methods. Hence, we can use CMA to offer deeper insights into how and why certain variables mediate the relationship between a cause and its outcome and to control for confounding factors.[45] Our results demonstrated the effectiveness of the mediation analysis because most of the identified cytokines and immune cells and some of the selected genes coincided with the results obtained with the correlation-based method. However, there were some genes that did not overlap between these two methods. The two approaches have different principles.[46] Considering the complex nature of the human immune system, genes that have obvious causal effects are more likely to play potentially important roles and exert direct effects than genes identified by correlation-based methods. In addition, correlation analysis is a statistical test used primarily to identify and explore linear relationships between only two variables. With CMA, we inferred the causal dependencies among the three omics datasets, and the identified factors jointly served as mediators of the immune response. However, there are also some problems to be solved. For example, given the treatment and covariates (i.e., the preexisting anti-Ad5 antibody titer and other physiological indexes), we cannot guarantee that the multiomics mediators are rigorously randomized. This problem results mainly from the unmeasured confounding factors that are related to this immune process. If the mediators are seriously imbalanced, then the estimated mediation effects will be inaccurate. In the future, an optional solution is to involve more auxiliary data/variables to alleviate the negative effect of unmeasured confounding factors, such as instrumental variables or negative controls.

There were several limitations of our study. The whole-blood transcriptome was studied to elucidate the immune features of Ad5-EBOV, and this approach has lower resolution than approaches using single-cell sequencing data. The latter may further reveal the immune activities of characteristic cells. We explored only the early correlates of the $GP_{1,2}$-specific IgG response. An extensive investigation of the Ebola-specific cellular immune response will better reveal the immune features of Ad5-vectored vaccines. Although immune signatures were obtained via correlation and causal analysis, further experimental verification is needed.

In conclusion, this study elucidated distinct Ad5-EBOV-induced signatures that correlated with the antibody response in subjects with different levels of preexisting anti-Ad5 antibodies. The antiviral and innate immune elements that exhibited an early response and were identified in three dimensions (genes, cytokines, and cell subsets) may be used to monitor effective vaccination and may serve as a guide for developing strategies to overcome preexisting immunity during the administration of Ad5-vectored vaccines.

MATERIALS AND METHODS

Study design

Thirty-six volunteers were recruited to receive 8×10^{10} viral particles (vp) of Ad5-EBOV, a replication-deficient human adenovirus-vectored vaccine encoding the glycoprotein of *Orthoebolavirus zairense*, which was approved for use by the China Food and Drug Administration on October 19, 2017. Blood samples were collected at 0, 1, 3, 7, and 28 days after vaccination. Plasma and peripheral blood mononuclear cell (PBMC) samples were isolated and saved at −80°C. The study was approved by the ethics committee of the Academy of Military Medical Science. All of the volunteers provided written informed consent to take part in the study.

Ebola $GP_{1,2}$-specific IgG assays

Nunc-Immuno 96-well plates were coated with 1 μg/mL *O. zairense* glycoprotein in Dulbecco's PBS and left at 4°C overnight. The plates were washed 6 times with PBS-Tween (PBS-T) and then blocked with casein for 1 h at room temperature (RT). Serum was diluted in casein to 1:100, 1:200, 1:500, 1:1,000, or 1:5,000 and added to the plate in triplicate. The plates were incubated for 2 h at RT and then washed as described previously. A secondary antibody (goat anti-human IgG conjugated to alkaline phosphatase; Sigma) was added at a

dilution of 1:1,000 in casein for 1 h at RT. The plates were subsequently washed and developed using 4-nitrophenyl phosphate in diethanolamine buffer (Pierce). The optical density (OD) was read at 405 nm using an ELx800 microplate reader.

We assessed $GP_{1,2}$-specific antibody responses against the vaccine-matched glycoprotein with ELISA, reported as the 90% effective concentration (EC_{90}; the concentration at which there is a 90% decrease in antigen binding), with subtraction of the prevaccination OD. The ELISA EC_{90} was measured at each time point, and the OD was read at 450 nm. A positive antibody response was defined as an ELISA EC_{90} value of at least 10. For ELISA EC_{90} values <10, a value of 5 was used for geometric mean titer (GMT) calculation.

Adenovirus neutralization assays

Anti-Ad5 NAb responses were assessed by a luciferase-based virus neutralization assay with an Ad5-luciferase system. Each sample was serially diluted 3-fold in duplicate from 1:12 to 1:8,748, and the diluent without serum was used as a negative control. Subsequently, 50 μL of each serum dilution was mixed and incubated with 50 μL of Ad5-luciferase at 1×10^7 vp/well for 1 h at 37°C. Next, 100 μL of 2×10^4 A549 cells was added to the mixture and incubated for 24 h at 37°C. Luciferase expression was detected using the Luciferase Assay System (Promega). The NAb titer was calculated as the reciprocal of the dilution for which luciferase activity was reduced by 90% of that of the negative control (IC_{90}) using nonlinear regression with four parameters in GraphPad Prism 8.0. A NAb titer of 200 was used to define the level of preexisting immunity according to previous studies.[9,47]

Luminex assays

Blood samples were centrifuged at 2,200 rpm for 7 min at 4°C. The upper plasma samples were isolated and kept at −70°C until use. The levels of 38 analytes were measured in duplicate plasma samples by a Luminex bead-based human cytokine/chemokine assay (Merck-Millipore) using Magpix equipment (Merck-Millipore) according to the manufacturer's instructions. The following analytes were measured: sCD40L, EGF, eotaxin/CCL11, FGF-2, Flt-3, fractalkine, G-CSF, GM-CSF, GRO, IFN-α2, IFN-γ, interleukin (IL)-1α, IL-1β, IL-1RA (receptor antagonist), IL-2, IL-3, IL-4, IL-5, IL-6, IL-7, IL-8, IL-9, IL-10, IL-12p40, IL-12p70, IL-13, IL-15, IL-17A, IFN-γ-induced protein 10 (IP-10), monocyte chemoattractant protein-1 (MCP-1), MCP-3, MDC, macrophage inflammatory protein (MIP)-1α, MIP-1β, TGF-α, tumor necrosis factor (TNF)-α, TNF-β, and VEGF. Standards were plotted and concentrations were determined using xPONENT software (version 4.2).

Flow cytometry

Cryopreserved PBMCs were thawed at 37°C and washed twice with RPMI 1640 (HyClone) supplemented with 10% fetal bovine serum (Gibco), 2 mM L-glutamine (Gibco), 100 U/mL penicillin, and 100 μg/mL streptomycin (Gibco) before use. PBMCs were blocked using human Fc block (BD Biosciences) and stained using the LIVE/DEAD Fixable Aqua Dead Cell Stain Kit (Invitrogen) for 30 min. Afterward, the PBMCs were stained for 30 min at 4°C with the following antibody cocktails: for analysis of DCs/monocytes, the cells were stained with anti-CD3-APC/Cy7 (UCHT1, 1:400, BioLegend), anti-CD19-APC/Cy7 (HIB19, 1:100, BioLegend), anti-CD56-APC/Cy7 (HCD56, 1:100, BioLegend), anti-HLA-DR-FITC (L243, 1:100, BioLegend), anti-CD14-BV510 (M5E2, 1:50, BioLegend), anti-CD16-AF700 (3G8, 1:100, BioLegend), anti-CD11c-APC (3.9, 1:50, BioLegend), anti-CD303-PerCP/Cy5.5 (201A, 1:50, BioLegend), anti-CD40-PE (5C3, 1:50, BioLegend), CD86-PE/Cy7 (IT2.2, 1:50, BioLegend), anti-CD83-BV421 (HB15e, 1:50, BioLegend), and anti-CCR7-BV605 (G043H7, 1:25, BioLegend) antibodies. For analysis of NK cells, cells were stained with two panels separately. The NK-1 panel included anti-CD3-APC/Cy7 (UCHT1, 1:400, BioLegend), anti-CD19-APC/Cy7 (HIB19, 1:100, BioLegend), anti-CD14-APC/Cy7 (HCD14, 1:100, BioLegend), anti-CD56-BV605 (HCD56, 1:50, BioLegend), anti-CD16-AF700 (3G8, 1:400, BioLegend), anti-NKp30-PE (P30-15, 1:50, BioLegend), anti-NKp46-PE/Cy7 (9E2, 1:50, BioLegend), anti-NKp44-BV510 (p44-8, 1:50, BD Biosciences), anti-2B40-APC (C1.7, 1:100, BioLegend), anti-CXC chemokine receptor 6 (CXCR6)-BV421 (K041E5, 1:50, BioLegend), anti-NKG2C-FITC (134591, 1:50, R&D Systems), and anti-CD57-PerCP/Cy5.5 (HNK-1, 1:50, BioLegend) antibodies. The NK-2 panel included anti-CD3-APC/Cy7 (UCHT1, 1:400, BioLegend), anti-CD19-APC/Cy7 (HIB19, 1:100, BioLegend), anti-CD14-APC/Cy7 (HCD14, 1:100, BioLegend), anti-CD56-BV605 (HCD56, 1:50, BioLegend), anti-CD16-AF700 (3G8, 1:400, BioLegend), anti-NKG2D-PerCP/Cy5.5 (1D11, 1:50, BioLegend), anti-CD69-PE/Cy7 (FN50, 1:50, BioLegend), anti-DNAM-1-APC (11A8, 1:100, BioLegend), anti-CD38 (HIT2, 1:50, BioLegend), anti-NKG2A-FITC (REA110, 1:50, Miltenyi), and anti-killer cell inhibitory receptor (KIR)-PE (HP-MA4, 1:200, BioLegend) antibodies. For analysis of B cells, the cells were stained with anti-CD3-APC/Cy7 (UCHT1, 1:400, BioLegend), anti-CD19-AF700 (SJ25C1, 1:100, BioLegend), anti-CD20-BV510 (2H7, 1:100, BioLegend), anti-CD24-BV605 (ML5, 1:100, BioLegend), anti-CD38-PE (HIT2, 1:100, BioLegend), anti-CD27-APC (O323, 1:100, BioLegend), anti-CD138-BV421 (MI15, 1:100, BioLegend), anti-IgD (IA6-2, 1:100, BioLegend), anti-CD69-PE/Cy7 (FN50, 1:50, BioLegend), and anti-CD80− PerCP/Cy5.5 (2D10, 1:50, Biosciences) antibodies. For analysis of T cells, the cells were stained with anti-CD19-APC/Cy7 (HIB19, 1:100, BioLegend), anti-CD14-APC/Cy7 (HCD14, 1:50, BioLegend), anti-CD3-Pacific Blue (OKT2, 1:400, BioLegend), anti-CD4-BV510 (RPA-T4, 1:50, BioLegend), anti-CD8a-PerCP/Cy5.5 (RPA-T8, 1:50, BioLegend), anti-HLA-DR-FITC (L243, 1:100, BioLegend), anti-CD38-PE (HIT2, 1:50, BioLegend), anti-CD45RA-AF700 (HI100, 1:400, BioLegend), anti-CD25-PE/Cy7 (BC96, 1:100, BioLegend), anti-CD127-APC (A019D5, 1:400, BioLegend), and anti-CCR7-BV605 (G043H7, 1:25, BioLegend) antibodies. Subsequently, the cells were washed twice and resuspended in 0.2 mL PBS. The data were collected using FACSCanto II (BD Biosciences) and FACSDiva version 8.0.1 software (BD Biosciences), and the FCS data files were further analyzed with FlowJo 10 software.

Bulk transcriptomic analysis

RNA was isolated from whole blood, and the purity of the RNA samples was determined with the NanoPhotometer (IMPLEN). The concentration and integrity of the RNA samples were detected by an Agilent 2100 RNA nano 6000 assay kit (Agilent Technologies). Sequencing libraries were generated using the VAHTS Universal V6 RNA-seq Library Prep Kit for Illumina (NR604-01/02), and index codes were added to attribute sequences to each sample. Clustering of the index-coded samples was performed on a cBot cluster generation system using the HiSeq PE Cluster Kit v4-cBot-HS (Illumina). After cluster generation, the libraries were sequenced on an Illumina platform, and 150-bp paired-end reads were generated. DESeq2 (version 1.38.3) in R 4.2.2 was used for differential gene analysis. Gene set enrichment analysis (GSEA) was performed using GSEA version 4.1.0 (http://www.gsea-msigdb.org/gsea). The correlation values between $GP_{1,2}$-specific IgG and day 1 versus day 0 gene expression were calculated as the Spearman correlation coefficient. Genes were ranked by R values and analyzed with GSEA using the blood transcription modules (BTMs)[48] to obtain BTM correlations with $GP_{1,2}$-specific IgG.

Causal mediation analysis (CMA)

CMA is a statistical approach used to investigate the underlying mechanisms through which a treatment affects an outcome variable.[49] It aims to understand the causal pathways or mediators that explain the relationship between the treatment and the outcome. The key idea in CMA is to decompose the total effect of treatment into two components: the direct effect and the indirect or mediation effect. The direct effect represents the effect of the treatment on the outcome that is not mediated through any intermediate variables, and the mediation effect represents the effect that operates through one or more mediators.

In this study, let T, Y, and M denote the treatment (ie, preexisting anti-Ad5 antibody titer), potential outcome (ie, $GP_{1,2}$-specific IgG titer), and mediator (ie, gene expression or cytokine concentration or immune cell response), respectively. Then, the direct effect can be defined as

$$\zeta_i(t) := Y_i(1, M_i(t)) - Y_i(0, M_i(t))$$

The indirect effect can be defined as

$$\delta_i(t) := Y_i(t, M_i(1)) - Y_i(t, M_i(0))$$

where i is the ID of a volunteer. Under the linearity assumption (ie, the treatment, outcome, mediator, and covariates obey linear functions), we immediately obtain the direct and indirect effects with the regression coefficients.

The proportion of the mediation effect on the total effect ($Proportion_{mediation\ effect}$) was used to measure the importance of one kind of gene/cytokine/cell in the immune response in this study.

$$Proportion_{mediation\ effect} = \frac{mediation\ \ effect}{direct\ \ effect + mediation\ \ effect}$$

In our study, the direct effect refers to the change in the titer of $GP_{1,2}$-specific antibodies induced by the EBOV itself. The indirect effect refers to the titer change of $GP_{1,2}$-specific antibodies induced by the genetic transcription, cytokines, or immune cells as mediators, which are activated by the EBOV.

Next, we present the assumptions required for our causal analysis and discuss their reasonability.

Assumption 1: stable unit treatment value assumption (SUTVA). The potential outcomes for any volunteer do not vary with the treatments assigned to other volunteers, and for each volunteer, there are no different forms or versions of each treatment level, which leads to different potential outcomes.

The SUTVA assumption indicates that each volunteer is independently assigned a treatment, (i.e., the preexisting anti-Ad5 antibody titer), and does not affect the outcomes of other volunteers. This condition is naturally satisfied in our empirical research. The preexisting

anti-Ad5 antibody titer is a preexisting physiological feature before the immune process, and it only affects each volunteer's own $GP_{1,2}$-specific antibody titer. Thus, each volunteer's outcome (i.e., the $GP_{1,2}$-specific antibody titer) was only determined by his own preexisting anti-Ad5 antibody titer, satisfying the SUTVA assumption.

Assumption 2: positivity. For volunteer i, given its observable confounders X_i, the possible treatments and mediators exist—in other words,

$$P(T_i = t|X_i = x) > 0,$$

$$P(\boldsymbol{M}_i(t) = \boldsymbol{m}|T_i = t, X_i = x),$$

for all of the possible t, x, and $\boldsymbol{m}$.

The positivity assumption indicates that both treatments (low or high preexisting anti-Ad5 antibody titer) are likely to be effective for all of the volunteers. Similarly, this assumption also holds in our setup. Specifically, our clinical trial data were drawn from two groups of people. Thus, unlike that in a generic observable study, the positivity assumption is strictly guaranteed here.

Assumption 3: sequential ignorability. Given the observable confounders X_i of volunteer i, we make the following assumptions:

$$\{Y_i(t', \boldsymbol{m}), M_i(t)\} \perp\!\!\!\perp T_i|X_i = x, \quad \text{(Equation 1)}$$

$$Y_i(t', \boldsymbol{m}) \perp\!\!\!\perp M_i(t)|T_i = t, X_i = x, \quad \text{(Equation 2)}$$

for all of the possible t, x, and $\boldsymbol{m}$.

Sequential ignorability aims to ensure that (1) the potential outcome and mediators are independent of the treatment assignment, given pretreatment covariates, and (2) the potential outcome is also independent of the mediators, given pretreatment covariates and ignorable treatment. Subassumption (1) is guaranteed under our experimental setup, because our clinical data follow the randomized controlled trial protocol; we randomly sampled volunteers from two groups regardless of their specific covariates. However, subassumption (2) may not always hold even in our randomized experiments. If subassumption (2) holds, then it indicates that among the volunteers who share the same treatment status and the same pretreatment characteristics, the mediators can be viewed as completely randomized. Moreover, although the subassumption (2) is nonrefutable,[50] it is commonly adopted by the CMA community.

Finally, we summarize the inputs and outputs of the CMA method here.

Input data:

- Preexisting anti-Ad5 antibody titer (as the treatment)
- $GP_{1,2}$-specific IgG titer (as the outcome)
- Sex (as a covariate)
- Age (as a covariate)
- Gene expression count (as a mediator)
- Cytokine concentration (as a mediator)
- Immune cell response (as a mediator)

Output data:

- Average mediation effect, including point estimation, p value, and confidence interval
- Average direct effect, including point estimation, p value, and confidence interval

Software and hardware platforms

Our hardware platform is shown as follows:

Central processing unit	Intel i9-10920X
Operating system	Ubuntu 18.04
Memory	128 GB
Graphics processing unit	RTX 3090*2

Our CMA was implemented with R language 4.3.1 and the open-source R package "mediation 4.5.0."

Statistical analysis

Statistical analysis was performed using GraphPad Prism (version 8.0) and R (version 4.2.2). Pearson and Spearman correlation coefficients were mainly used to quantify the correlation between the measured values in this study. Principal-component analysis (PCA) was performed to evaluate the correlation and differences between samples in the low Ad5 NAb cohort (LAC) and high Ad5 NAb cohort HAC using a permutational multivariate analysis of variance test based on Bray-Curtis distance measures.[51] The Wilcoxon matched-paired signed rank test and Mann-Whitney test were used to compare differences between different time points or groups. The false discovery rate (FDR) method was used to adjust p values for multiple comparisons. p values or FDR adjusted p values are presented in the indicated figures as appropriate (*$p < 0.05$; **$p < 0.01$; ***$p < 0.001$).

DATA AND CODE AVAILABILITY

The raw sequence data have been deposited in the Genome Sequence Archive in the National Genomics Data Center (GSA-Human: HRA004935). All of the other data are available in the main text or the supplemental information.

REFERENCES

1. Tatsis, N., and Ertl, H.C.J. (2004). Adenoviruses as vaccine vectors. Mol. Ther. **10**(4): 616–629. https://doi.org/10.1016/j.ymthe.2004.07.013.
2. Chang, J. (2021). Adenovirus Vectors: Excellent Tools for Vaccine Development. Immune Netw. **21**(1): e6. https://doi.org/10.4110/in.2021.21.e6.
3. Cheng, C., Gall, J.G.D., Kong, W.P., et al. (2007). Mechanism of ad5 vaccine immunity and toxicity: fiber shaft targeting of dendritic cells. PLoS Pathog. **3**(2): e25. https://doi.org/10.1371/journal.ppat.0030025.
4. Zhu, F.C., Wurie, A.H., Hou, L.H., et al. (2017). Safety and immunogenicity of a recombinant adenovirus type-5 vector-based Ebola vaccine in healthy adults in Sierra Leone: a single-centre, randomised, double-blind, placebo-controlled, phase 2 trial. Lancet **389**(10069): 621–628. https://doi.org/10.1016/s0140-6736(16)32617-4.
5. Dolzhikova, I.V., Zubkova, O.V., Tukhvatulin, A.I., et al. (2017). Safety and immunogenicity of GamEvac-Combi, a heterologous VSV- and Ad5-vectored Ebola vaccine: An open phase I/II trial in healthy adults in Russia. Hum. Vaccines Immunother. **13**(3): 613–620. https://doi.org/10.1080/21645515.2016.1238535.
6. Guo, Q., Chan, J.F.W., Poon, V.K.M., et al. (2018). Immunization With a Novel Human Type 5 Adenovirus-Vectored Vaccine Expressing the Premembrane and Envelope Proteins of Zika Virus Provides Consistent and Sterilizing Protection in Multiple Immunocompetent and Immunocompromised Animal Models. J. Infect. Dis. **218**(3): 365–377. https://doi.org/10.1093/infdis/jiy187.
7. Baden, L.R., Stieh, D.J., Sarnecki, M., et al. (2020). Safety and immunogenicity of two heterologous HIV vaccine regimens in healthy, HIV-uninfected adults (TRAVERSE): a randomised, parallel-group, placebo-controlled, double-blind, phase 1/2a study. Lancet. HIV **7**(10): e688–e698. https://doi.org/10.1016/s2352-3018(20)30229-0.
8. Jacob-Dolan, C., and Barouch, D.H. (2022). COVID-19 Vaccines: Adenoviral Vectors. Annu. Rev. Med. **73**: 41–54. https://doi.org/10.1146/annurev-med-012621-102252.
9. Zhu, F.C., Hou, L.H., Li, J.X., et al. (2015). Safety and immunogenicity of a novel recombinant adenovirus type-5 vector-based Ebola vaccine in healthy adults in China: preliminary report of a randomised, double-blind, placebo-controlled, phase 1 trial. Lancet **385**(9984): 2272–2279. https://doi.org/10.1016/s0140-6736(15)60553-0.
10. Zhu, F.C., Li, Y.H., Guan, X.H., et al. (2020). Safety, tolerability, and immunogenicity of a recombinant adenovirus type-5 vectored COVID-19 vaccine: a dose-escalation, open-label, non-randomised, first-in-human trial. Lancet **395**(10240): 1845–1854. https://doi.org/10.1016/s0140-6736(20)31208-3.
11. Malik, S., Kishore, S., Nag, S., et al. (2023). Ebola Virus Disease Vaccines: Development, Current Perspectives & Challenges. Vaccines **11**(2): 268. https://doi.org/10.3390/vaccines11020268.
12. Fausther-Bovendo, H., and Kobinger, G.P. (2014). Pre-existing immunity against Ad vectors: humoral, cellular, and innate response, what's important? Hum. Vaccines Immunother. **10**(10): 2875–2884. https://doi.org/10.4161/hv.29594.
13. Seregin, S.S., and Amalfitano, A. (2009). Overcoming pre-existing adenovirus immunity by genetic engineering of adenovirus-based vectors. Expet Opin. Biol. Ther. **9**(12): 1521–1531. https://doi.org/10.1517/14712590903307388.
14. Roberts, D.M., Nanda, A., Havenga, M.J.E., et al. (2006). Hexon-chimaeric adenovirus serotype 5 vectors circumvent pre-existing anti-vector immunity. Nature **441**(7090): 239–243. https://doi.org/10.1038/nature04721.
15. Croyle, M.A., Patel, A., Tran, K.N., et al. (2008). Nasal delivery of an adenovirus-based vaccine bypasses pre-existing immunity to the vaccine carrier and improves the immune response in mice. PLoS One **3**(10): e3548. https://doi.org/10.1371/journal.pone.0003548.
16. Barouch, D.H., Pau, M.G., Custers, J.H.H.V., et al. (2004). Immunogenicity of recombinant adenovirus serotype 35 vaccine in the presence of pre-existing anti-Ad5 immunity. J. Immunol. **172**(10): 6290–6297. https://doi.org/10.4049/jimmunol.172.10.6290.
17. Iwasaki, A., and Medzhitov, R. (2015). Control of adaptive immunity by the innate immune system. Nat. Immunol. **16**(4): 343–353. https://doi.org/10.1038/ni.3123.
18. Rhee, E.G., Blattman, J.N., Kasturi, S.P., et al. (2011). Multiple innate immune pathways contribute to the immunogenicity of recombinant adenovirus vaccine vectors. J. Virol. **85**(1): 315–323. https://doi.org/10.1128/jvi.01597-10.
19. Collignon, C., Bol, V., Chalon, A., et al. (2020). Innate Immune Responses to Chimpanzee Adenovirus Vector 155 Vaccination in Mice and Monkeys. Front. Immunol. **11**: 579872. https://doi.org/10.3389/fimmu.2020.579872.

20. Ye, Y., Zhang, Y., Yang, N., et al. (2022). Profiling of immune features to predict immunotherapy efficacy. Innovation **3**(1): 100194. https://doi.org/10.1016/j.xinn.2021.100194.
21. Provine, N.M., Amini, A., Garner, L.C., et al. (2021). MAIT cell activation augments adenovirus vector vaccine immunogenicity. Science **371**(6528): 521–526. https://doi.org/10.1126/science.aax8819.
22. Shen, C.F., Yen, C.L., Fu, Y.C., et al. (2022). Innate Immune Responses of Vaccinees Determine Early Neutralizing Antibody Production After ChAdOx1nCoV-19 Vaccination. Front. Immunol. **13**: 807454. https://doi.org/10.3389/fimmu.2022.807454.
23. Raeven, R.H.M., van Riet, E., Meiring, H.D., et al. (2019). Systems vaccinology and big data in the vaccine development chain. Immunology **156**(1): 33–46. https://doi.org/10.1111/imm.13012.
24. Rappuoli, R., Siena, E., and Finco, O. (2018). Will Systems Biology Deliver Its Promise and Contribute to the Development of New or Improved Vaccines? Systems Biology Views of Vaccine Innate and Adaptive Immunity. Cold Spring Harbor Perspect. Biol. **10**(8): a029256. https://doi.org/10.1101/cshperspect.a029256.
25. Kazmin, D., Nakaya, H.I., Lee, E.K., et al. (2017). Systems analysis of protective immune responses to RTS,S malaria vaccination in humans. Proc. Natl. Acad. Sci. USA **114**(9): 2425–2430. https://doi.org/10.1073/pnas.1621489114.
26. Pinski, A.N., and Messaoudi, I. (2020). To B or Not to B: Mechanisms of Protection Conferred by rVSV-EBOV-GP and the Roles of Innate and Adaptive Immunity. Microorganisms **8**(10): 1473. https://doi.org/10.3390/microorganisms8101473.
27. Arunachalam, P.S., Scott, M.K.D., Hagan, T., et al. (2021). Systems vaccinology of the BNT162b2 mRNA vaccine in humans. Nature **596**(7872): 410–416. https://doi.org/10.1038/s41586-021-03791-x.
28. Pinschewer, D.D. (2017). Virally vectored vaccine delivery: medical needs, mechanisms, advantages and challenges. Swiss Med. Wkly. **147**: w14465. https://doi.org/10.4414/smw.2017.14465.
29. Bottermann, M., Foss, S., van Tienen, L.M., et al. (2018). TRIM21 mediates antibody inhibition of adenovirus-based gene delivery and vaccination. Proc. Natl. Acad. Sci. USA **115**(41): 10440–10445. https://doi.org/10.1073/pnas.1806314115.
30. Zak, D.E., Andersen-Nissen, E., Peterson, E.R., et al. (2012). Merck Ad5/HIV induces broad innate immune activation that predicts CD8⁺ T-cell responses but is attenuated by preexisting Ad5 immunity. Proc. Natl. Acad. Sci. USA **109**(50): E3503–E3512. https://doi.org/10.1073/pnas.1208972109.
31. McElroy, A.K., Erickson, B.R., Flietstra, T.D., et al. (2014). Biomarker correlates of survival in pediatric patients with Ebola virus disease. Emerg. Infect. Dis. **20**(10): 1683–1690. https://doi.org/10.3201/eid2010.140430.
32. Bergamaschi, C., Terpos, E., Rosati, M., et al. (2021). Systemic IL-15, IFN-γ, and IP-10/CXCL10 signature associated with effective immune response to SARS-CoV-2 in BNT162b2 mRNA vaccine recipients. Cell Rep. **36**(6): 109504. https://doi.org/10.1016/j.celrep.2021.109504.
33. Tian, Y., Seumois, G., De-Oliveira-Pinto, L.M., et al. (2019). Molecular Signatures of Dengue Virus-Specific IL-10/IFN-γ Co-producing CD4 T Cells and Their Association with Dengue Disease. Cell Rep. **29**(13): 4482–4495.e4. https://doi.org/10.1016/j.celrep.2019.11.098.
34. Huttner, A., Combescure, C., Grillet, S., et al. (2017). A dose-dependent plasma signature of the safety and immunogenicity of the rVSV-Ebola vaccine in Europe and Africa. Sci. Transl. Med. **9**(385): eaaj1701. https://doi.org/10.1126/scitranslmed.aaj1701.
35. Takano, T., Morikawa, M., Adachi, Y., et al. (2022). Distinct immune cell dynamics correlate with the immunogenicity and reactogenicity of SARS-CoV-2 mRNA vaccine. Cell Rep. Med. **3**(5): 100631. https://doi.org/10.1016/j.xcrm.2022.100631.
36. Rechtien, A., Richert, L., Lorenzo, H., et al. (2017). Systems Vaccinology Identifies an Early Innate Immune Signature as a Correlate of Antibody Responses to the Ebola Vaccine rVSV-ZEBOV. Cell Rep. **20**(9): 2251–2261. https://doi.org/10.1016/j.celrep.2017.08.023.
37. Rinchai, D., Deola, S., Zoppoli, G., et al. (2022). High-temporal resolution profiling reveals distinct immune trajectories following the first and second doses of COVID-19 mRNA vaccines. Sci. Adv. **8**(45): eabp9961. https://doi.org/10.1126/sciadv.abp9961.
38. Ryan, F.J., Norton, T.S., McCafferty, C., et al. (2023). A systems immunology study comparing innate and adaptive immune responses in adults to COVID-19 mRNA and adenovirus vectored vaccines. Cell Rep. Med. **4**(3): 100971. https://doi.org/10.1016/j.xcrm.2023.100971.
39. Huang, M., Zheng, H., Tan, W., et al. (2023). Molecular Signatures in Swine Innate and Adaptive Immune Responses to African Swine Fever Virus Antigens p30/p54/CD2v Expressed Using a Highly Efficient Semliki Forest Virus Replicon System. Int. J. Mol. Sci. **24**(11): 9316. https://doi.org/10.3390/ijms24119316.
40. Haralambieva, I.H., Oberg, A.L., Dhiman, N., et al. (2012). High-dimensional gene expression profiling studies in high and low responders to primary smallpox vaccination. J. Infect. Dis. **206**(10): 1512–1520. https://doi.org/10.1093/infdis/jis546.
41. Sun, Z., Ke, L., Zhao, Q., et al. (2023). The use of bioinformatics methods to identify the effects of SARS-CoV-2 and influenza viruses on the regulation of gene expression in patients. Front. Immunol. **14**: 1098688. https://doi.org/10.3389/fimmu.2023.1098688.
42. Li, S., Zhu, Z., Yang, F., et al. (2021). Porcine Epidemic Diarrhea Virus Membrane Protein Interacted with IRF7 to Inhibit Type I IFN Production during Viral Infection. J. Immunol. **206**(12): 2909–2923. https://doi.org/10.4049/jimmunol.2001186.
43. Dong, H., Wu, W., Li, J., et al. (2022). PML Body Component Sp100A Is a Cytosolic Responder to IFN and Activator of Antiviral ISGs. mBio **13**(6): e0204422. https://doi.org/10.1128/mbio.02044-22.
44. Brodin, P., and Davis, M.M. (2017). Human immune system variation. Nat. Rev. Immunol. **17**(1): 21–29. https://doi.org/10.1038/nri.2016.125.
45. Imai, K., Keele, L., and Tingley, D. (2010). A general approach to causal mediation analysis. Psychol. Methods **15**(4): 309–334. https://doi.org/10.1037/a0020761.
46. Rubin, D.B. (2005). Causal Inference Using Potential Outcomes: Design, Modeling, Decisions. J. Am. Stat. Assoc. **100**(March): 322–331. https://doi.org/10.1198/016214504000001880.
47. Wang, B., Li, J., Wu, S., et al. (2023). A seroepidemiological survey of adenovirus type 7 circulation among healthy adults in China and in Sierra Leone, West Africa. Front. Public Health **11**: 1095343. https://doi.org/10.3389/fpubh.2023.1095343.
48. Li, S., Rouphael, N., Duraisingham, S., et al. (2014). Molecular signatures of antibody responses derived from a systems biology study of five human vaccines. Nat Immunol **15**(2): 195–204. https://doi.org/10.1038/ni.2789.
49. Böhnke, J.R. (2016). Explanation in causal inference: Methods for mediation and interaction. Q. J. Exp. Psychol. **69**(6): 1243–1244. https://doi.org/10.1080/17470218.2015.1115884.
50. Manski, C.F. (2007). Identification for Prediction and Decision (Harvard University Press), p. 368. https://doi.org/10.4159/9780674033665.
51. Anderson, M.J. (2017). Permutational Multivariate Analysis of Variance (PERMANOVA) (Wiley StatsRef: Statistics Reference Online), pp. 557–574. https://doi.org/10.1002/9781118445112.stat07841.

ACKNOWLEDGMENTS

We thank all of the volunteers for engaging in this study. This study was funded by the National Natural Science Foundation of China 31900671.

AUTHOR CONTRIBUTIONS

Conceptualization: W.C., L.H., Z.Z., and W.Y.; methodology: Z.Z., Z.C., H.C., S.W., W.Z., Y.W., N.H., and X.S.; investigation: S.W., R.J., B.W., and L.X.; visualization: Z.C. and H.C.; funding acquisition: W.C. and Z.Z.; project administration: Z.Z. and W.Y.; supervision: W.C., L.H., and J.Z.; writing – original draft: Z.Z., W.Y., Z.C., and H.C.; writing – review & editing: all authors.

DECLARATION OF INTERESTS

The authors declare no competing interests.

SUPPLEMENTAL INFORMATION

It can be found online at https://doi.org/10.1016/j.xinn.2024.100603.